ResearchGate

See discussions, stats, and author profiles for this publication at: https://www.researchgate.net/publication/229522346

Ignition and oxidation of 1-hexene/toluene mixtures in a shock tube and a jet-stirred reactor: Experimental and kinetic modeling study

ARTICLE *in* INTERNATIONAL JOURNAL OF CHEMICAL KINETICS · SEPTEMBER 2007

Impact Factor: 1.52 · DOI: 10.1002/kin.20265

CITATIONS
10

READS
15

6 AUTHORS, INCLUDING:

Mohammed Yahyaoui
AGI
14 PUBLICATIONS **236** CITATIONS
SEE PROFILE

Nabiha Chaumeix
CNRS Orleans Campus
76 PUBLICATIONS **806** CITATIONS
SEE PROFILE

Claude Etienne Paillard
Université d'orléans & CNRS-ORLEANS (ICARE)
79 PUBLICATIONS **968** CITATIONS
SEE PROFILE

Available from: Mohammed Yahyaoui
Retrieved on: 26 January 2016

Author Proof

Ignition and Oxidation of 1-Hexene/Toluene Mixtures in a Shock Tube and a Jet-Stirred Reactor: Experimental and Kinetic Modeling Study

M. YAHYAOUI,[1] N. DJEBAÏLI-CHAUMEIX,[1] P. DAGAUT,[1] C.-E. PAILLARD,[1]
B. HEYBERGER,[2] G. PENGLOAN[3]

[1]CNRS, *Laboratoire de Combustion et des Systèmes Réactifs*, 1C, *Avenue de la Recherche Scientifique*, 45071 *Orléans Cedex 2*, *France*
[2]TOTAL/RM/STD/RECH/CRES, *Centre de Recherche de Solaize Nouveaux Carburants & Véhicules*, BP 22-69360 *Solaize*, *France*
[3]PSA *Peugeot Citroën*, *Engine and Transmission System Design*, *Fuels and Systems Chemistry*, *Gasoline and Diesel*, 18 *Rue des Fauvelles*, 92256 *La Garenne Colombes Cedex*, *France*

Received 14 March 2006; revised 15 December 2006, 28 February 2007; accepted 6 March 2007

DOI 10.1002/kin.20265
Published online in Wiley InterScience (www.interscience.wiley.com).

ABSTRACT: The oxidation of several binary mixtures 1-hexene/toluene has been investigated both in a shock tube and in a jet-stirred reactor (JSR). The self-ignition behavior of binary mixtures was compared to that of neat hydrocarbons studied under the same conditions. Furthermore, molecular species concentration profiles were measured by probe-sampling and GC/MS, FID, TCD analyses for the oxidation of the mixtures in a JSR. Experiments were carried out over the temperature range 750–1860 K. Mixtures were examined under two pressures 0.2 and 1 MPa, with 0.1% initial concentration of fuel. The equivalence ratio was varied from 0.5 to 1.5. The experiments were modeled using a detailed chemical kinetic reaction mechanism. The

Correspondence to: Nabiha Djebaïli-Chaumeix; e-mail: Chaumeix@cnrs-orleans.fr.
Contract grant sponsor: CNRS-SPI.
Contract grant sponsor: TOTAL.
Contract grant sponsor: PSA.
Q1 Contract grant sponsor: La Région Centre in the framework of ARC "Formation des Polluants Automobiles."
© 2007 Wiley Periodicals, Inc.

WILEY InterScience® DISCOVER SOMETHING GREAT

Author Proof

modeling study showed that interactions between hydrocarbons submechanisms were not limited to small reactive radicals. Other types of interactions involving hydrocarbon fragments derived from the oxidation of the fuel components must be considered. These interactions mainly consist of hydrogen abstraction reactions. For example, benzyl radical that is the major radical produced from the oxidation of toluene at high temperature can abstract hydrogen from 1-hexene and their products such as hexenyl radicals. Similarly, propyl, allyl, and hexenyl radicals that are the major radicals produced during 1- hexene oxidation at high temperature can abstract hydrogen from toluene. Improved modeling was achieved when such interaction reactions were included in the model. Good agreement between experimental and calculated data was obtained using the proposed detailed chemical kinetic scheme. © 2007 Wiley Periodicals, Inc. Int J Chem Kinet 39: 1–21, 2007

INTRODUCTION

Gasoline is a complex mixture of a large number of different hydrocarbons (aromatics, alkanes, olefins, naphthenes, oxygenates). Their combustion in car engines yields emission of many pollutants (volatile organic compounds, NO_X, SO_X, PAH, and so on). In order to preserve human health and environment, governments in Europe, America, and Japan imposed strict regulations to control exhaust gas from engines. In response to the increasingly constraining standards of pollutants emission, it is necessary to have accurate description of hydrocarbons oxidation for a better prediction of pollutants emission.

In this work, mixtures of two constituents of gasoline have been chosen: 1-hexene for olefins and toluene for aromatics. The neat oxidation of hydrocarbons has been the subject of a large number of studies, but few kinetic data are available for the oxidation of hydrocarbons mixtures besides natural gas surrogates [1].

1-Hexene is among the major olefin formed during the oxidation of higher alkanes such as *n*-decane or *n*-hexadecane [1]. This compound can also be produced during *n*-heptane steam cracking or oxidation and cyclohexane pyrolysis. 1-Hexene research octane number is equal to 76 [2]. Its structure includes a long paraffinic tail, the double bond being at the end. So its oxidation includes both linear paraffin and olefin behaviors. Several studies of the oxidation of light olefins have been presented [3–10]. However, few studies have dealt with the kinetics of oxidation of large olefins like 1-hexene. 1-Hexene has been investigated at low temperature [11], by pressure–time measurements between 500 and 560 K. 1-Hexene kinetics of decomposition was studied using, respectively, a shock tube and a very low pressure pyrolysis experiment [12, 13]; both studies determined unimolecular and retroene constant rate reactions. The ignition and oxidation products of 1-hexene and *n*-hexane in an engine were compared [14]. 1-Hexene oxidation and autoignition were investigated at low temperature in a rapid compression machine [15], between 630 and 850 K, and the influence of the double bond position on hexenes chemistry was examined. Ignition delay times of 1-hexene were measured in a shock tube at high temperature [16], and a detailed chemical kinetics was generated automatically. More recently, 1-hexene was studied in soot-forming nonpremixed flames [17].

Aromatic hydrocarbons have become an important constituent of gasoline because of their high-energy density and their high-antiknock rating. The combustion of aromatic hydrocarbons is still far from being fully understood. Toluene is one of the smallest and simplest aromatic molecules. Ignition delay times of toluene were measured at high temperature between 1300 and 1880 K in a shock tube [18–20]. The reaction of toluene with molecular oxygen was studied behind reflected shock waves [21], by following benzyl radical formation. The oxidation of toluene was investigated in a turbulent flow reactor at 1200 K [22]. The pathways of benzaldehyde formation from benzyl radical were investigated [23]. The pathways of toluene oxidation were examined in more detail [24,25] from experiments performed in a flow reactor at atmospheric pressure. Toluene oxidation in a jet-stirred reactor at atmospheric pressure and between 1100 and 1400 K was investigated by Ristori et al. [26], and a detailed kinetic mechanism for its oxidation was established. The toluene/air burning velocities were measured at 1 [27] and 3 atm [28]. Toluene oxidation was studied using a single pulse shock tube at high pressure (up to 600 bar) [29], and an improved chemical kinetics was elaborated to simulate species mole fractions. The thermal decomposition of toluene in benzyl radicals at high temperatures was carried out in a shock tube [30–33], and a rate constant for this reaction was determined.

Concerning the experimental studies for the oxidation of binary liquid fuel mixtures, one can find a limited number of papers; most of them focusing on primary reference fuels isooctane/*n*-heptane mixtures.

Author Proof

The autoignition tendencies of several binary primary reference fuels were investigated in an atmospheric flow reactor between 570 and 920 K [34]. The reactivity of primary reference fuel blends was examined in a motored research engine by measuring exhaust manifold carbon monoxide concentration [35]. Leppard [36] studied the oxidation of isooctane/*n*-heptane mixtures, and the effect of high-octane olefins: 2-butene and 1,3-butadiene, on isooctane oxidation in a motored engine. Dagaut et al. [37] studied the oxidation of isooctane/*n*-heptane in a JSR at high pressure (10 atm) and over a wide range of temperatures (550–1150 K).

Very few studies concern the oxidation of toluene mixtures with other hydrocarbons. The effect of toluene on *n*-heptane reactivity was carried out by measuring CO concentration, from the oxidation of several toluene/*n*-heptane mixtures [34]. Klotz et al. [38] studied the cooxidation of toluene/*n*-butane blends in an atmospheric flow reactor at 1200 K. Recently, the autoignition of *n*-heptane/toluene mixtures was investigated in a single cylinder engine [39]. Ignition delay times of 1-hexene/toluene (30/70) mixtures were measured in a rapid compression machine below 900 K [40], and compared to those of pure 1-hexene, showing that 1-hexene ignites at a temperature lower than that at which the binary mixtureignites, and some species mole fractions were measured: toluene, 1-hexene, butyloxirane, pentanal, 1,3-hexadiene, methylvinyloxetane, benzaldehyde, benzene, heptenylbenzene, and dibenzyl.

For the modeling of hydrocarbons mixtures experiments, some authors [14,38,41,42] assembled hydrocarbons submechanisms, assuming that interactions between fuel components were limited to radical pool effects, and that each component of the mixture reacts via parallel mechanisms and only interactions including small reactive radicals (H, O, OH, HO_2, CH_3) are possible. Other works reported that cross-reactions are very important and must be added. In this way, Tanaka et al. [43] showed that ignition delay of primary reference fuels in rapid compression machine (273–393 K, 0.75–1 bar) is simulated better by adding a simple interaction between isooctane and *n*-heptane: $C_8H_{18} + C_7H_{15} = C_8H_{17} + C_7H_{16}$. More recently, Andrae et al. [39] showed an improvement in ignition delay times simulation of primary reference fuels as well as *n*-heptane/toluene mixtures in a shock tube at high pressure (40 bars), by adding cross-reactions such as $RH + R_1^{\bullet} = R^{\bullet} = R_1H$ and $R_1OO^{\bullet} + RH = R_1OOH + R^{\bullet}$. Naik et al. [44] confirmed the importance of cross-reactions to predict autoignition and heat release rate of surrogate fuels for gasoline.

EXPERIMENTAL SETUP

Shock Tube

A series of experiments were performed behind reflected shock waves. A shock tube with a 0.9-m long stainless steel high pressure driver section and a 4-m long stainless steel low pressure driven section with a 78-mm internal diameter was used. Reactive mixtures were diluted with argon. Both sections of the shock tube were evacuated using two primary vacuum pumps. The shock velocity was measured via four pressure transducers equally spaced by 150 mm, mounted flush with the inner surface of the tube, the last one being 10 mm before the shock tube end wall. A fused silica window (9 mm optical diameter and 6 mm thickness) was mounted across a 306-nm filter, which is characteristic of OH emission, and equipped with an UV-sensitive photomultiplier tube (R928-HAMMAMATSU). Both pressure and emission signals were transferred and registered using digital oscilloscope. Reflected shock conditions (P_5, T_5) were calculated from the standard procedure [45].

For the ignition delay time measurements at high pressure (1 MPa), a mixture of N_2 and He was used as driver gas. This procedure allowed an increase in the observation time and the measurement of longer ignition delay times. This was particularly useful in the lower temperature range of this study.

The reactive gas mixtures were prepared manometrically using 1-C_6H_{12} (Aldrich, +99%), toluene (Aldrich, 99.8%), O_2 (Air Liquide, 99.999%) Ar (Air Liquide, 99.999%), and N_2 (Air Liquide, +99.99%) in a 10-L Pyrex bulb. The liquid hydrocarbon was degassed several times before the mixtures were prepared. The mixtures were mechanically mixed for 1–2 h to ensure homogeneous composition.

Figure 1 shows an example of the recorded signals, representing pressure evolution and OH emission. The experimental ignition delay time is defined as the time between the passage of the reflected shock wave (indicated by a pressure jump), monitored by pressure transducer (0.2 μs time response), and 50% of the maximum OH emission signal at 306 nm delivered by the photomultiplier (3 ns time response).

Jet-Stirred Reactor

The high pressure, jet-stirred reactor experimental setup is that presented earlier by Dagaut et al. [46]. A jet-stirred reactor (JSR) consisting of a fused silica sphere with an inside volume of 39 cm^3 was used. It

Author Proof

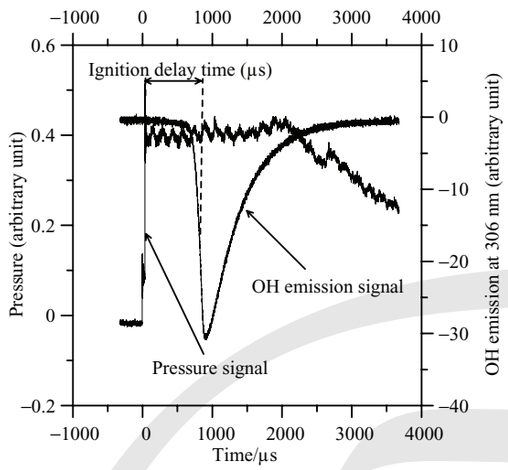

Figure 1 Evolution of the pressure and emission signals recorded by the oscilloscope as a function of the time. 0.1% (toluene/1-hexene)(30/70)/0.9% O_2/99% Ar; $\phi = 1$; $T_5 = 1480$ K; $P_5 = 0.215$ MPa.

is equipped with 4 nozzles of 1 mm inner diameter admitting the reactant gases that achieve the stirring. It is surrounded by two independent insulted heating wires and located inside a stainless steel pressure-resistant jacket filled with insulating material. It can operate at pressures as high as 4 MPa. Pressure in the outer part of the JSR is balanced by a regulated nitrogen flow. All the gases are delivered by mass flow controllers. The liquid fuel is initially delivered by a high pressure liquid chromatography pump to an atomizer–vaporizer assembly maintained at 423 K, providing a homogeneous dilutant (nitrogen)–fuel gas mixture. To prevent reactions before the entrance of the reactor, the reactive mixture is delivered through a capillary, up to the mixing point before the entrance of the injectors. In order to prevent temperature gradients in the JSR, all the gases are preheated to the working temperature before injection, using a 12.5-kW induction heating system. Two regulated heating wires of 1 kW each are used to maintain the temperature of the upper and lower parts of the reactor to the desired working temperature. Temperature gradients were checked by moving a quartz isolated Pt-Pt/Rh-10% thermocouple and found <2 K cm^{-1}. Low-pressure samples (80 Torr) were analyzed online and collected in 1 L Pyrex bulbs for further off-line GC-TCD-FID and GC/MS analyses.

Experiments have been performed at a constant mean residence time of 0.5 s at a pressure of 1 MPa. Temperature was varied between 750 and 1200 K. A high level of dilution was used (0.1% of fuel) to reduce the temperature gradient in the JSR. The sampling procedure was carried out using a low pressure sonic probe inside the reactor. Two types of analyses were performed in this work: (i) online GC analyses (GC/MS and GC/FID) of condensable products and (ii) off-line analyses of low-pressure samples (80 Torr) collected in Pyrex bulbs (1 L) evacuated beforehand to stop reactions advancement. For the off-line analyses, we used CG-FID for C_1–C_7 hydrocarbons, CG-TCD-FID for O_2, CO, CO_2, and CH_2O, with a detection limit equal to 1 ppm. Helium was used as a carrier gas in these analyses. For hydrogen analyses by TCD, nitrogen was used as a carrier gas. Identification and quantification of species were accomplished by using standard gas mixtures. GC/MS analyses were carried out to identify initially unknown chromatographic peaks. From JSR experiments, species measured are C_7H_8 (toluene), 1-C_6H_{12} (1-hexene), O_2, CO, CO_2, H_2, CH_4, C_2H_4, C_2H_2, C_2H_6, C_3H_6, 1-C_4H_8, 1,3-C_4H_6, C_6H_6, C_6H_5CHO (benzaldehyde), $C_6H_5CHCH_2$ (styrene), and $C_6H_5C_2H_5$ (ethyl benzene). The carbon balance was checked for every sample and found good within 10% error.

The experimental conditions in a shock tube and in a JSR are listed in Table I.

EXPERIMENTAL

Ignition

Ignition delay times of binary mixtures 1-hexene/toluene with different mole fractions (10/90, 50/50, 70/30, and 90/10) were measured. Comparing ignition delay times of binary mixtures with those of pure hydrocarbons measured in the same conditions showed that ignition delay times of toluene are the longest one, whereas those of 1-hexene are the shortest

Table I Experimental Conditions During 1-Hexene/Toluene Oxidation Performed in a JSR and in a Shock Tube

	1-C_6H_{12}	C_7H_8	O_2	N_2 or Ar	ϕ	T (K)	P (MPa)
JSR	0.03	0.07	0.6–1.8	98.1–99.3	0.5–1.5	750–1170	1
Shock tube	0.01–0.09	0.01–0.09	0.9	99	1	1360–1860	0.2–1

Reactants are expressed in mole percent.

Author Proof

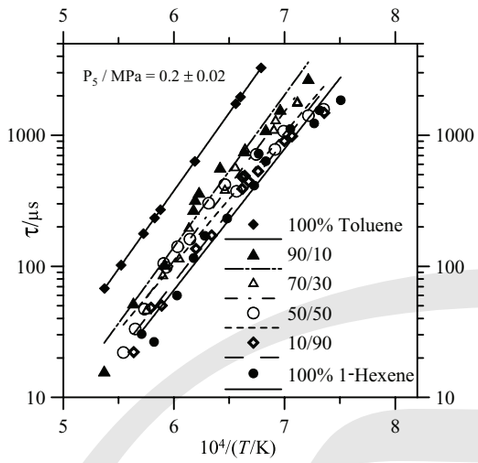

Figure 2 Comparison of ignition delay times measured for binary mixtures, 1-hexene/toluene (10/90, 30/70, 50/50, 90/10) and neat hydrocarbons, 0.1% fuel/ 0.9% O_2/ 99% Ar; $\phi = 1$; $P_5 = 0.2 \pm 0.02$ MPa.

one. Binary mixture ignition delay times are located between those of neat hydrocarbons. So, toluene is the less reactive hydrocarbon, whereas 1-hexene is the most reactive one. Binary mixtures are more reactive than toluene and less reactive than 1-hexene, and ignition delay time of binary mixtures increases with increase in the initial toluene concentration as one can see in Fig. 2 (Table II summarizes experimental data obtained in a shock tube). In Table III, we compared the heat of some unimolecular reactions occurred during 1-hexene and toluene oxidations, as well as the heat formation at 300 K of the different species implied. Calculations were made using CHEMThermo [47]. These computations show that the lower value for 1-hexene dissociations concerns the reaction: 1-C_6H_{12} = 1,3-C_6H_{11} + H ease by the presence of the double bond, with a value equal to 82.49 kcal/mol at 300 K, whereas for toluene the lower heat of C—H fission corresponds to the reaction: $C_7H_8 = C_6H_5CH_2 + H$, corresponding to H atom dissociation from a methyl group, with a value of 90.47 kcal/mol at 300 K, so 8 kcal/mol higher than the fission of C—H bond in 1-Hexene. For the C—C bonds break, the lower value concerns the reaction: 1-C_6H_{12} = a-C_3H_5 + n-C_3H_7 with 72.73 kcal/mol at 300 K, while for toluene molecule, the heat of C—C fission reaction is equal to 102.32 kcal/mol at 300 K, so about 30 kcal/mol higher than 1-hexene, which confirms that bond strengths of C—H as well as C—C bonds are weaker in 1-hexene molecule than in toluene. In fact, bond strength influences ignition delay times [48]. 1-Hexene bonds break easily and increase radicals pool that favors ignition. So mixtures containing high 1-hexene concentration ignite faster (see Fig. 2).

Figure 3 presents the measured ignition delay times of binary mixtures at a fixed temperature versus 1-hexene mole fraction in the fuel mixture. This figure shows that binary mixtures' ignition delay times do not vary linearly with the mole fraction of 1-hexene in the fuel mixture. Thus, the oxidation pathways for the binary mixture 1-hexene/toluene are more complicated than a simple combination of their oxidation submechanisms. This indicates that chemical kinetic interactions between hydrocarbons fragments occur. Vanhove et al. [40] showed the same trends by

Table II Shock Tube Experimental Data Obtained

1-C_6H_{12}	C_7H_8	O_2	Ar	T (K)	τ (μs)
	For a pressure around 0.2 MPa			1367	1550
				1418	1117
				1464	634
				1478	722
				1487	413
0.001	0	0.009	0.99	1543	232
				1593	171
				1619	116
				1659	60
				1718	26
				1752	30
				1359	1480
				1415	983
				1429	904
				1479	531
				1498	444
				1506	491

Continued

Author Proof

Table II Continued

1-C_6H_{12}	C_7H_8	O_2	Ar	T (K)	τ (μs)
0.0009	0.0001	0.009	0.99	1511	391
				1511	480
				1577	172
				1613	136
				1698	50
				1726	48
				1774	22
				1360	1578
				1386	1414
				1430	1074
				1447	779
				1483	714
				1523	374
				1548	420
0.0005	0.0005	0.009	0.99	1584	303
				1627	161
				1657	141
				1686	98
				1693	105
				1744	47
				1770	33
				1804	22
				1405	1780
				1406	1748
				1445	1287
				1449	1090
				1505	780
0.0003	0.0007	0.009	0.99	1526	564
				1548	379
				1630	195
				1653	114
				1695	85
				1738	46
				1386	2710
				1437	1580
				1464	1107
				1507	760
				1558	572
0.0001	0.0009	0.009	0.99	1606	368
				1615	324
				1619	271
				1690	104
				1775	52
				1862	16
				1473.22	3265
				1524.82	1738
				1615.69	632
0	0.001	0.009	0.99	1701.02	270
				1716.55	233
				1746.55	178
				1810.64	102
				1861.17	68

Continued

Author Proof

Table II Continued

1-C_6H_{12}	C_7H_8	O_2	Ar	T (K)	τ (μs)
		For a pressure around 1 MPa			
				1431	775
				1473	515
				1543	201
				1577	138
0.0003	0.007	0.009	0.99	1622	136
				1622	96
				1646	89
				1670	81
				1690	49
				1867	11

T is the reflected shock temperature.
τ is the autoignition delay time.
The reactants are given in mole fraction.

comparing ignition delay times and cool flame measurements in a rapid compression machine of 1-hexene and 1-hexene/toluene (70/30) mixture.

Species Profiles

Mole fractions of molecular species formed during the oxidation of binary mixtures 1-hexene/toluene (30/70) were measured for different equivalence ratios and temperatures at 1 MPa and at constant mean residence time (0.5 s). In this study, major species produced directly from 1-hexene oxidation such as propene (C_3H_6) and 1-butene (1-C_4H_8) and from the oxidation of toluene such as benzaldehyde (C_6H_5CHO) and styrene ($C_6H_5CHCH_2$) were measured. However, no other species resulting from a combination of large radicals were identified, like heptenyl benzene mentioned by Vanhove et al. [40], and resulting from the cross-termination reaction between benzyl radical produced during toluene oxidation and hexenyl radicals formed by 1-hexene consumption. Figure 4 shows major species measured during 1-hexene/ toluene (30/70)

Table III The Heat of Unimolecular Reactions of 1-Hexene and Toluene Used in This Work and the Heat of Formation of the Corresponding Species

Species	ΔH_f (kcal/mol) at 300 K	Species	Unimolecular Reactions	ΔH_r (kcal/mol) at 300 K
H	52.11		1-C_6H_{12} = 1,1-C_6H_{11} + H	109.5
CH_3	34.84		1-C_6H_{12} = 1,2-C_6H_{11} + H	108.39
C_2H_3	71.8		1-C_6H_{12} = 1,3-C_6H_{11} + H	82.49
C_2H_5	28	1-C_6H_{12}	1-C_6H_{12} = 1,4-C_6H_{11} + H	98.7
pC_4H_9	17.92		1-C_6H_{12} = 1,5-C_6H_{11} + H	99.11
a-C_3H_5	38.68		1-C_6H_{12} = 1,6-C_6H_{11} + H	108.39
n-C_3H_7	24.05		1-C_6H_{12} = C_2H_3 + pC_4H_9	99.72
1-C_4H_7	46.04		1-C_6H_{12} = a-C_3H_5 + n-C_3H_7	72.73
1-C_5H_{11}	14.1		1-C_6H_{12} = 1-C_4H_7 + C_2H_5	84.04
1-C_6H_{12}	−10		1-C_6H_{12} = 1-C_5H_9 + CH_3	87.86
1,1-C_6H_{11}	47.39	C_7H_8	C_7H_8 = $C_6H_5CH_2$ + H	90.47
1,2-C_6H_{11}	46.28		C_7H_8 = C_6H_5 + CH_3	102.32
1,3-C_6H_{11}	20.38			
1,4-C_6H_{11}	36.59			
1,5-C_6H_{11}	36.99			
1,6-C_6H_{11}	38.09			
1-C_5H_{11}	43.02			
C_6H_5	79.48			
$C_6H_5CH_2$	50.36			
C_7H_8	12			

Author Proof

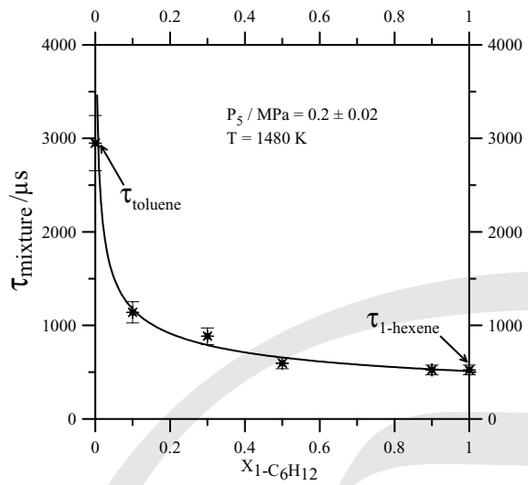

Figure 3 Ignition delay times of binary mixtures versus 1-hexene initial mole fraction in the fuel. $T = 1480$ K and $P_5 = 0.2 \pm 0.02$ MPa.

oxidation in a jet-stirred reactor at stoichiometric equivalence ratio.

Comparing 1-hexene mole fractions obtained from the oxidation of pure 1-hexene and a 1-hexene/toluene mixture at stoichiometric equivalence ratio shows that 1-hexene starts to react at higher temperature when toluene is present, as can be seen from Fig. 5. This figure also shows that 1-hexene mole fraction decrease is more drastic when oxidized alone than when toluene is present.

The effect of toluene on 1-hexene oxidation is demonstrated by comparing the rates of consumption of 1-hexene alone and in the presence of toluene. As shown in Fig. 6 when normalized rate at a given temperature is defined as follows:

$$\text{Rate } (\text{s}^{-1}) = -1/\tau((([1\text{-}C_6H_{12}]_{\text{measured}} - [1\text{-}C_6H_{12}]_{\text{injected}})/[1\text{-}C_6H_{12}]_{\text{injected}})$$

the rate of consumption of 1-hexene is greater when oxidized alone than in the presence of toluene. Also we can see that the inhibition of 1-hexene oxidation by toluene is negligible at temperatures greater than 950 K. As shown by the shock tube study, 1-hexene is more reactive than toluene. So, 1-hexene starts to react first becoming the far greater contributor to the developing radical pool. Furthermore, the two fuel components simultaneously compete for the available radicals. A simplified ratio of the reaction rates was calculated using hydrocarbon mole fractions measured experimentally, to illustrate competitive reactions between hydrocarbons mixture components and small reactive radicals such as OH, H, and O. Consider, for example, the reaction of hydrocarbons with OH radical. OH attacks toluene according to the reaction

$$\text{R758} : C_7H_8 + \text{OH} = C_6H_5CH_2 + H_2O$$
$$\left(\frac{\text{d}[C_7H_8]}{\text{d}t}\right) = -k_{758}[C_7H_8][\text{OH}]$$

while the OH radical reacts with 1-hexene by H abstraction to form several hexenyl radicals, and by addition to the double bond according to the reactions:

$$\text{R1000–1003} : 1\text{-}C_6H_{12} + \text{OH} = 1, i\text{-}C_6H_{11} + H_2O$$

(where $i = 3$, 4, 5, or 6 and represents radical site position with regard to the double bond).

$$\text{R1015} : 1\text{-}C_6H_{12} + \text{OH} = C_5H_{11} + CH_2O$$
$$\left(\frac{\text{d}[1\text{-}C_6H_{12}]}{\text{d}t}\right) = -(k_{1000} + k_{1001} + k_{1002} + k_{1003} + k_{1015}[1\text{-}C_6H_{12}][\text{OH}]$$

A ratio of these rate expressions was calculated from

$$\frac{\text{Rate}_{\text{toluene+OH}}}{\text{Rate}_{1-\text{hexene+OH}}} = \frac{k_{758}[C_7H_8]}{(k_{1000} + k_{1001} + k_{1002} + k_{1003} + k_{1015})[1\text{-}C_6H_{12}]}$$

This ratio neglects reverse reactions, because of the large concentration of the fuel components relative to their associated reaction products. Since fuel species concentrations were measured experimentally, the ratio can be calculated as a function of temperature. Similar ratios were determined for the reactions of both hydrocarbon with O, H, and O_2.

The relative reactions rate calculations are plotted as a function of temperature in Fig. 7. This figure shows that toluene reacts with small labile radicals at rates comparable to or greater than 1-hexene. If the decay of 1-hexene was in fact driven by abstraction reactions (mainly by OH radical [49]), at low temperature (<950 K) and as shown in its flow diagram performed at 900 K and 1 MPa in a JSR (Fig. 8), toluene present in the fuel mixture would consume small radicals and inhibits the decay of 1-hexene. Toluene reactions with these radicals mainly yield a benzyl radical as demonstrated by their flow diagrams at both 900 and 1100 K (Figs. 9 and 10); the benzyl radical is stabilized by resonance, and so very few reactive, it inhibits the oxidation of the mixture as noticed under shock tube conditions (Fig. 1). For temperatures greater than 950 K, 1-hexene

Author Proof

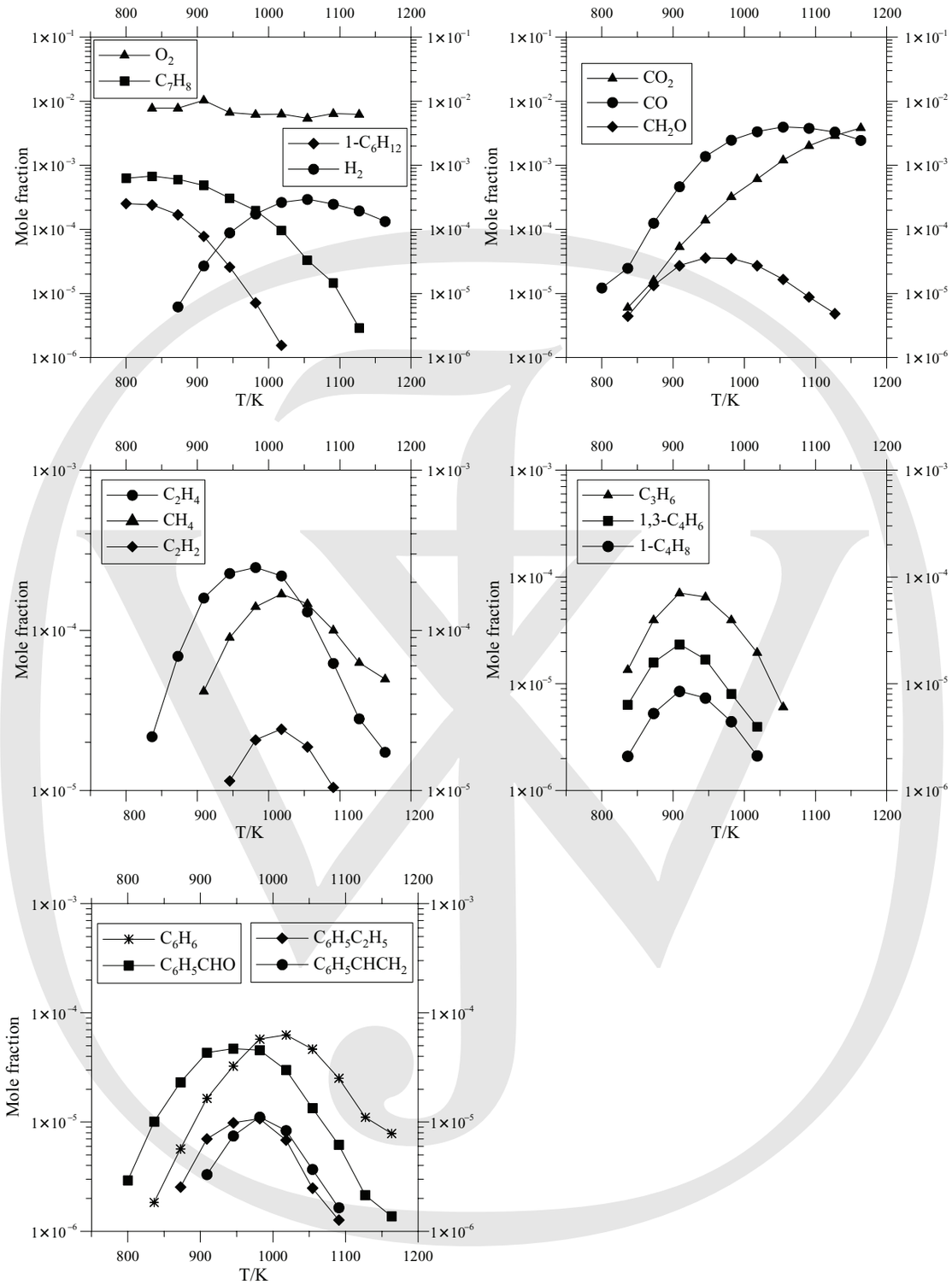

Figure 4 Mole fractions of major species measured within the oxidation of the binary mixture 1-hexene/toluene (30/70) in a JSR (0.1% fuel/ 0.9% O_2/ 99% N_2; $\tau = 0.5$ s; $\phi = 1$; $P = 1$ MPa).

Author Proof

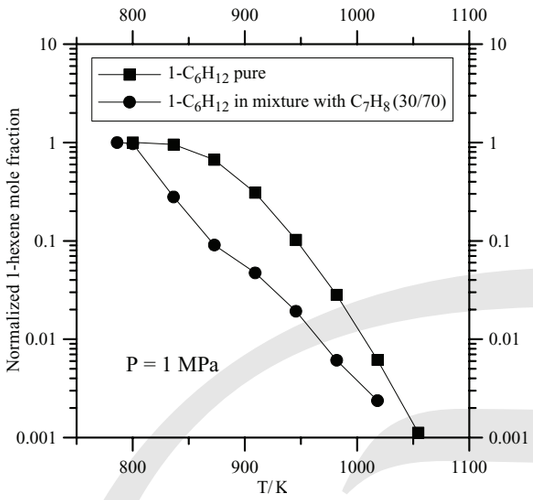

Figure 5 Comparison of normalized 1-hexene mole fractions when oxidized alone and in the presence of toluene in a JSR (0.1% fuel/ 0.9% O_2/ 99% N_2; $\tau = 0.5$ s; $\phi = 1$; $P =$ 1 MPa).

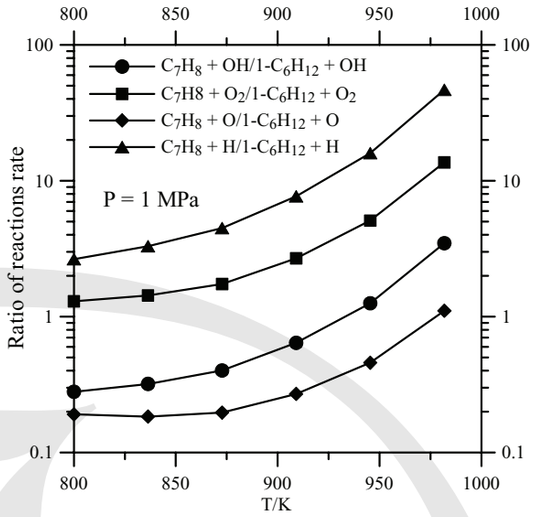

Figure 7 Ratio of rates of reaction of small labile radicals with the fuel components of the mixture 1-hexene/toluene (30/70) in a jet-stirred reactor (0.1% fuel/ 0.9% O_2/ 99% N_2; $\tau = 0.5$s; $\phi = 1$; $P = 1$ MPa).

is mainly consumed through thermal decomposition as can be seen from its flow diagram performed at 1100 K and 1 MPa (Fig. 11) yielding allyl (a-C_3H_5) and propyl (n-C_3H_7) radicals. Therefore, in this temperature range ($T > 950$ K), its decay becomes partially independent of radical attacks and unaffected by the presence of toluene (Fig. 6).

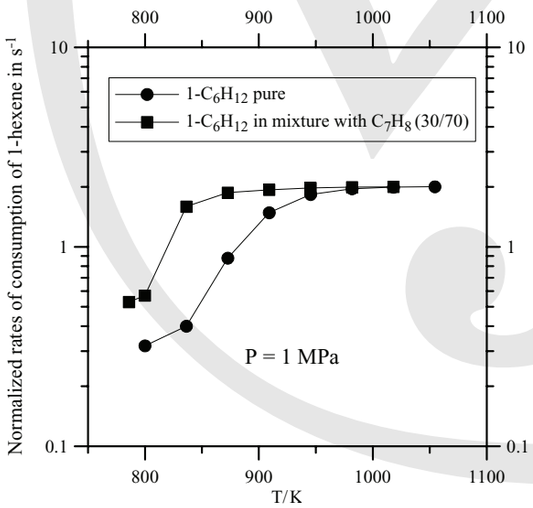

Figure 6 Comparison of 1-hexene rates of consumption when oxidized alone and in the presence of toluene in a JSR (0.1% fuel/ 0.9% O_2/ 99% N_2; $\tau = 0.5$ s; $\phi = 1$; $P = 1$ MPa).

Modeling

The ignition delays were computed using the SENKIN computer code [50], assuming the constant volume approximation was valid. For the modeling of the species profiles obtained from JSR experiments, we used the PSR computer code [51].

The kinetic mechanism elaborated by Dagaut [1] was used as a starting point. This mechanism designed for high-temperature range contains toluene submechanism and was validated on concentration profiles obtained from toluene oxidation in a JSR experiments between 1000 and 1400 K at 0.1 MPa as well as on ignition delay times measured in a shock tube between 1400 and 2000 K at 0.2 MPa While for 1-hexene oxidation, we adopted the kinetic mechanism elaborated by Yahyaoui et al. [49], validated on JSR experiments at 1 MPa between 750 and 1100 K, and on ignition delay times measured on shock tube between 1310 and 1870 K under two pressures 0.2 and 1 MPa. Constant rate of falloff reactions was taken into account when information was available. The rate constants for the reverse reactions were computed from the forward rate constants and the appropriate equilibrium constants calculated using thermochemical data [1,52].

The added interaction reactions are those of hexenyl radicals attacking on toluene (R1027–R1030) to produce benzyl and 1-hexene. Reactions between 1,3-C_6H_{11} and benzyl, which are among the major radicals

Author Proof

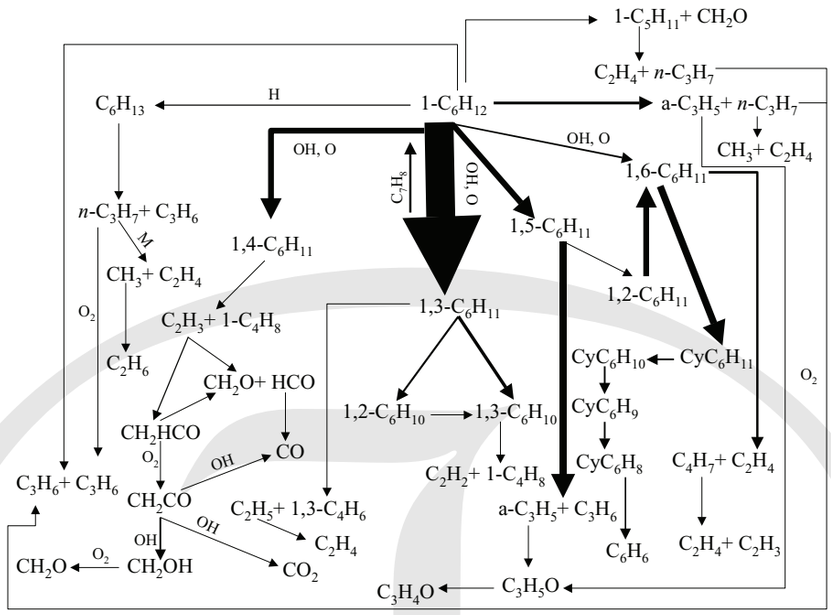

Figure 8 Reaction paths for 1-hexene consumption during the oxidation of the mixture 1-hexene/toluene (30/70); 0.1% fuel/0.9% O_2/99% N_2; $\phi = 1$; 1 MPa at 900 K in a JSR.

formed here, to yield hexadienes and toluene, were also included

R1027–R1030 : 1, i-$C_6H_{11} + C_7H_8 = 1\text{-}C_6H_{12} + C_6H_5CH_2$

R1031 : 1, 3-$C_6H_{11} + C_6H_5CH_2 = 1$, 2-$C_6H_{10} + C_7H_8$

R1032 : 1, 3-$C_6H_{11} + C_6H_5CH_2 = 1$, 3-$C_6H_{10} + C_7H_8$

The resulting mechanism involves 159 species and 1242 reversible reactions. Comparison between the

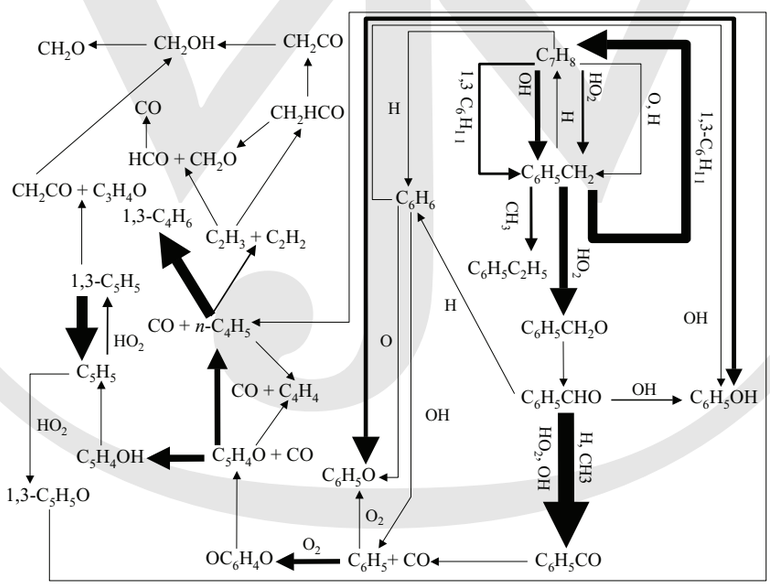

Figure 9 Reaction paths for toluene consumption during the oxidation of the mixture 1-hexene/ toluene (30/70); 0.1% fuel/0.9% O_2/99% N_2; $\phi = 1$; 1 MPa at 900 K in a JSR.

Author Proof

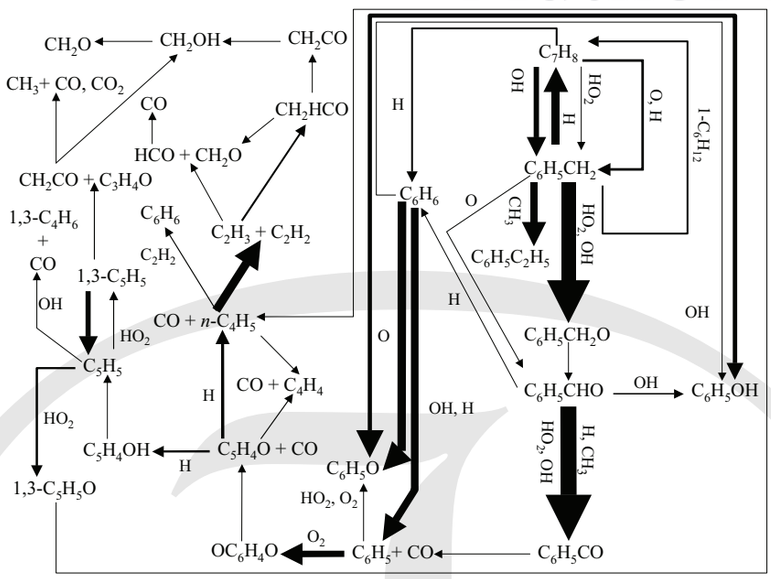

Figure 10 Reaction paths for toluene consumption during the oxidation of the mixture 1-hexene/toluene (30/70); 0.1% fuel/0.9% O_2/99% N_2; $\phi = 1$; 1 MPa at 1100 K in a JSR.

JSR experimental data and the model predictions is shown in Figs. 12–14. As shown, a simple combination of the chemical kinetic reaction submechanisms for the two fuel components is not sufficient to simulate well our experiments. So interactions involving large radicals, especially resonance-stabilized radicals, such as benzyl and 1,3-C_6H_{11} produced by the oxidation of toluene and 1-hexene, respectively, need to be added to the combination of toluene and 1-hexene kinetic submechanisms. When the cross-reactions mentioned above are omitted, the reactivity of both 1-hexene and toluene is overestimated, which also affects the

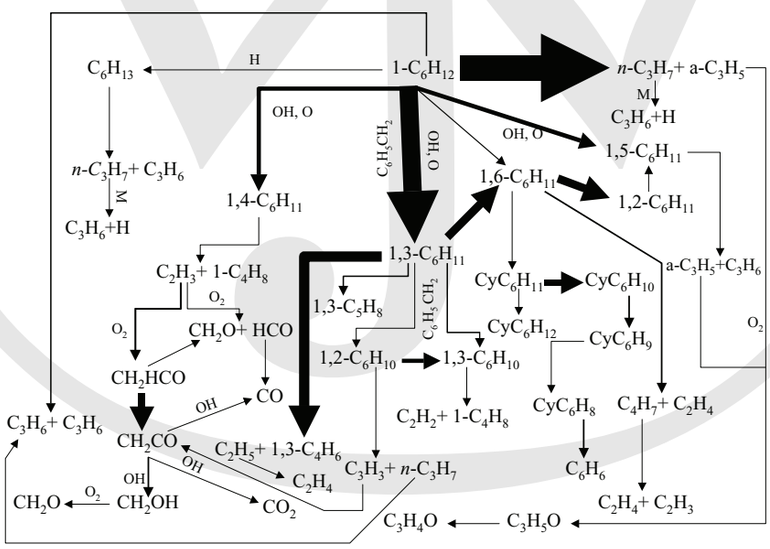

Figure 11 Reaction paths for 1-hexene consumption during the oxidation of the mixture 1-hexene/toluene (30/70); 0.1% fuel/0.9% O_2/99% N_2; $\phi = 1$; 1 MPa at 1100 K in a JSR.

Author Proof

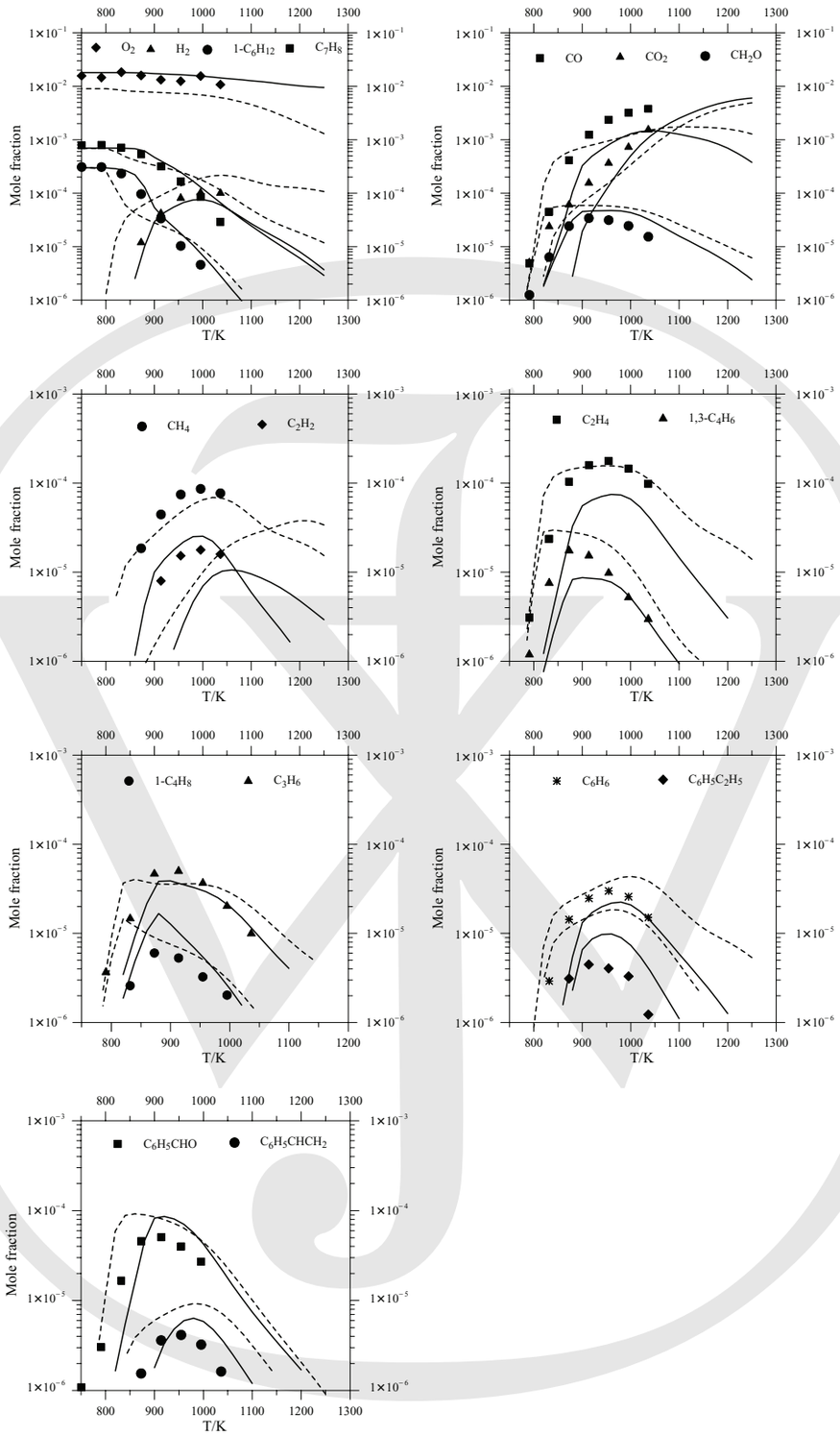

Figure 12 Comparison between experimental data (symbols) and modeling results (lines) for the oxidation of the binary mixture 1-hexene/toluene (30/70) in a JSR (0.1% fuel/ 1.8% O_2/ 98.1% N_2; $\phi = 0.5$; $P = 1$ MPa; $\tau = 0.5$ s). The solid line: full mechanism; the dotted line: without added cross-reactions.

Author Proof

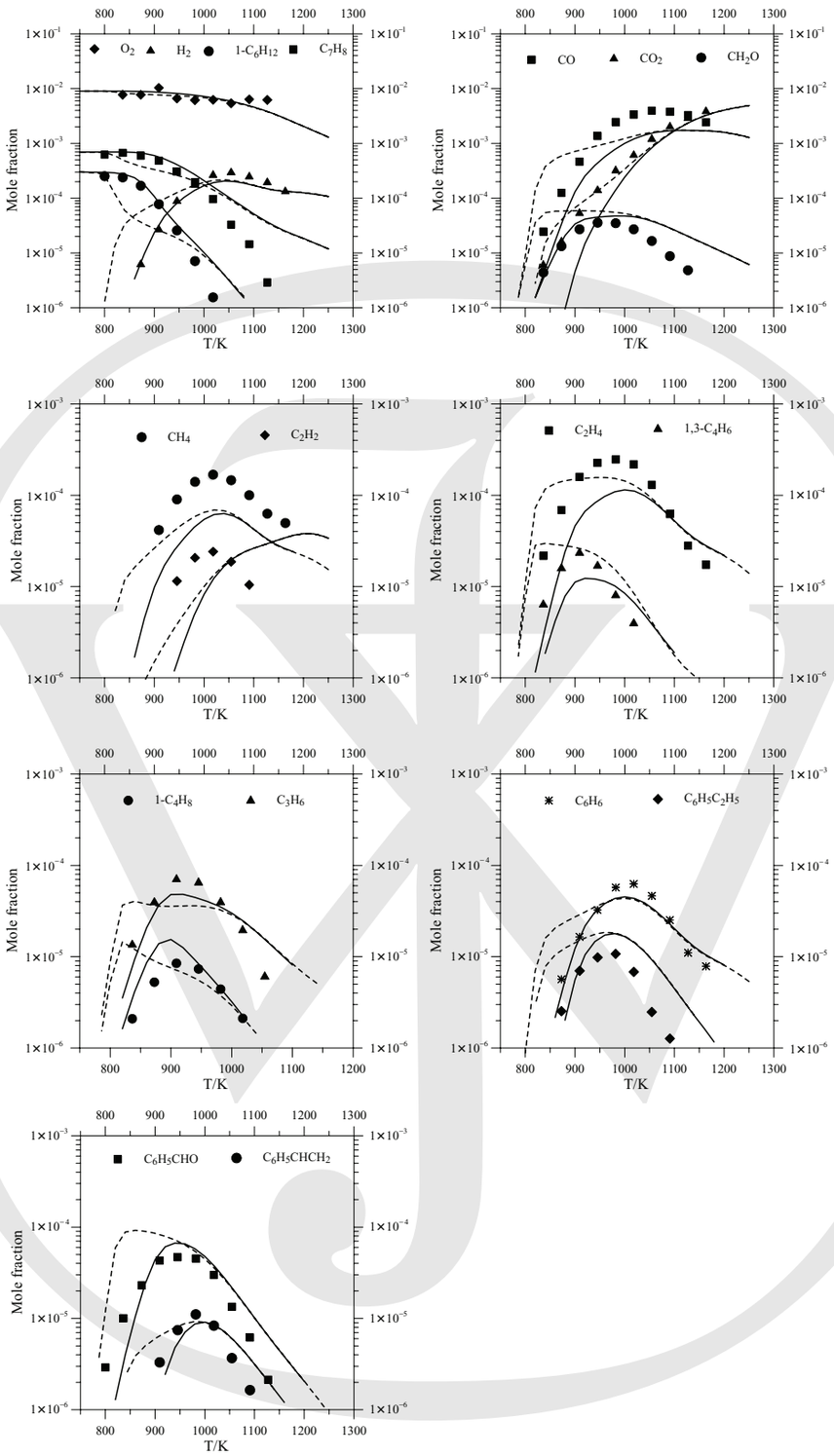

Figure 13 Comparison between experimental data (symbols) and modeling results (lines) for the oxidation of the binary mixture 1-hexene/toluene (30/70) in a JSR (0.1% fuel/ 0.9% O_2/99% N_2; $\phi = 1$; $P = 1$ MPa; $\tau = 0.5$ s). The solid line: full mechanism; the dotted line: without added cross-reactions.

Author Proof

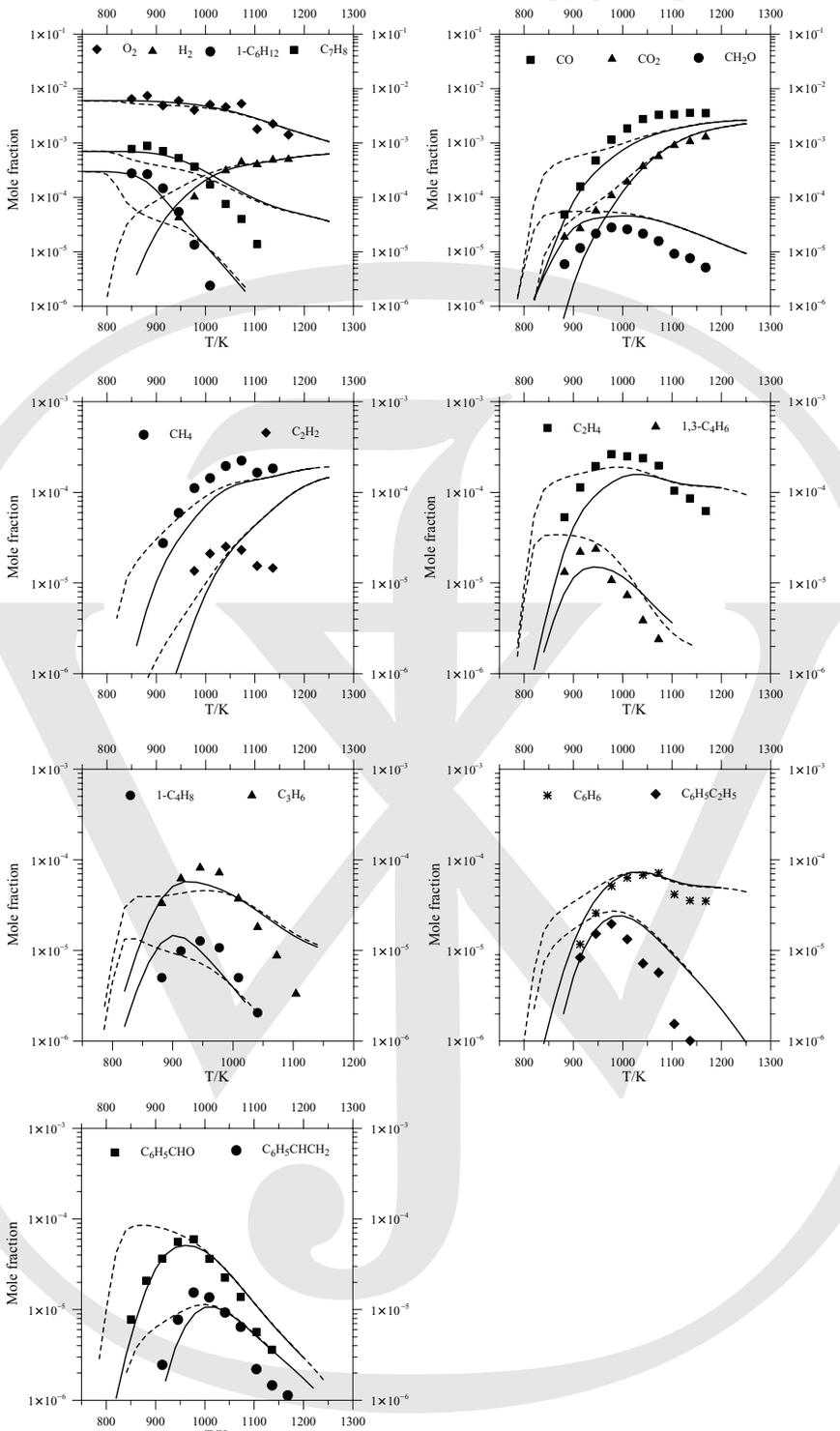

Figure 14 Comparison between experimental data (symbols) and modeling results (lines) for the oxidation of the binary mixture 1-hexene/toluene (30/70) in a JSR (0.1% fuel/ 0.6% O_2/ 99.3 N_2; $\phi = 1.5$; $P = 1$ MPa; $\tau = 0.5$ s). The solid line: full mechanism; the dotted line: without added cross-reactions.

Author Proof

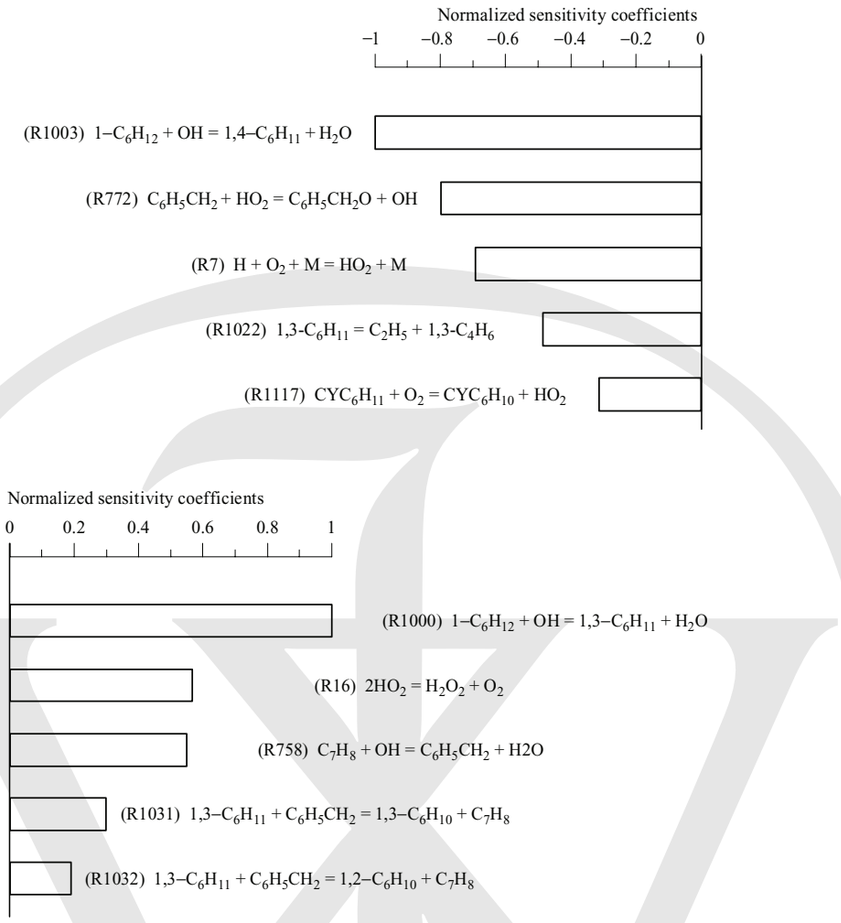

Figure 15 Sensitivity analysis of 1-hexene consumption in the mixture 1-hexene/toluene (30/70) in a JSR, 0.1% fuel/0.9% O2/99% N_2; $\tau = 0.5$s; $\phi = 1$; $P = 1$ MPa; $T = 900$ K.

other computed mole fractions. Species formation is predicted at earlier temperatures than experimentally found. Adding interaction reactions improves calculated mole fraction of the two hydrocarbons and of all species. The modeling improvement is more pronounced under rich and stoichiometric conditions. For fuel-lean condition ($\phi = 0.5$), CO, CO_2, CH_4, and C_2H_4 are better predicted when cross-reactions are omitted, while their concentrations are underpredicted when cross-reactions are added. On the other hand, under the same conditions, the mole fraction of reactants (toluene, 1-hexene, oxygen) is better predicted with the full mechanism, containing cross-reactions, as well as other species produced from 1-hexene such as C_3H_6, 1-C_4H_8, and all the species resulting from toluene oxidation, i.e., benzene, ethyl benzene, styrene, and benzaldehyde. In fact, under lean conditions, small reactive radicals are formed in high quantity, so interactions between hydrocarbon submechanisms via these radicals are important and may be sufficient to describe cross-reactions between toluene and 1-hexene. Acetylene simulation is bad, and some modeling improvements are needed.

Sensitivity analyses were performed for 1-C_6H_{12}/C_7H_8 (30/70), in a JSR at 900 K and stoichiometric equivalence ratio. Concerning 1-hexene consumption (Fig. 15), the main promoting reaction is R1003 that forms 1,4-C_6H_{11}, while the most inhibiting reaction is R1000 producing 1,3-C_6H_{11} which in turn can recycle 1-hexene through reaction R1027 by abstraction of H radical from benzyl radical. Among the reactions inhibiting 1-hexene oxidation, one finds reaction R758 from toluene submechanism, through which toluene consumes the OH radical at the expense of

Author Proof

Table IV Rate Expressions for Reactions Discussed in This Work

Reaction	Rate Expression		
	log A	n	E_a
R6: $H + O_2 = OH + O$	14.27	0	16812
R755: $C_7H_8 = C_6H_5CH_2 + H$	15.47	0	88194
R758: $C_7H_8 + OH = C_6H_5CH_2 + H_2O$	13	0	2180
R760: $C_7H_8 + H = C_6H_5CH_2 + H_2$	14.69	0	12499
R770: $C_6H_5CH_2 = C_5H_5 + C_2H_2$	13.78	0	70000
R1000: 1-$C_6H_{12} + OH = 1,3$-$C_6H_{11} + H_2O$	13.77	0	1230
R1001: 1-$C_6H_{12} + OH = 1,6$-$C_6H_{11} + H_2O$	5.45	2.3	236
R1002: 1-$C_6H_{12} + OH = 1,5$-$C_6H_{11} + H_2O$	6.8	2	−500
R1003: 1-$C_6H_{12} + OH = 1,4$-$C_6H_{11} + H_2O$	6.8	2	−500
R1015: 1-$C_6H_{12} + OH = C_5H_{11} + CH_2O$	11	0	−4000
R1022: 1,3-$C_6H_{11} = 1,3$-$C_4H_6 + C_2H_5$	10.6	0	38250
R1027: 1,3-$C_6H_{11} + C_7H_8 = 1$-$C_6H_{12} + C_6H_5CH_2$	12.6	0	3760
R1028: 1,4-$C_6H_{11} + C_7H_8 = 1$-$C_6H_{12} + C_6H_5CH_2$	11	0	9514
R1029: 1,5-$C_6H_{11} + C_7H_8 = 1$-$C_6H_{12} + C_6H_5CH_2$	11	0	9514
R1030: 1,6-$C_6H_{11} + C_7H_8 = 1$-$C_6H_{12} + C_6H_5CH_2$	11	0	9514
R1031: 1,3-$C_6H_{11} + C_6H_5CH_2 = 1,3$-$C_6H_{10} + C_7H_8$	12.2	0	0
R1032: 1,3-$C_6H_{11} + C_6H_5CH_2 = 1,2$-$C_6H_{10} + C_7H_8$	12	0	0

Q2 Total rate $k = AT^n \exp(-E_a/RT)$, units: s, mol, cm^3, cal, K.

1-hexene.

$$\text{R1003}: 1\text{-}C_6H_{12} + OH = 1,4\text{-}C_6H_{11} + H_2O$$

$$\text{R1000}: 1\text{-}C_6H_{12} + OH = 1,3\text{-}C_6H_{11} + H_2O$$

$$\text{R1027}: 1,3\text{-}C_6H_{11} + C_7H_8 = 1\text{-}C_6H_{12} + C_6H_5CH_2$$

$$\text{R758}: C_7H_8 + OH = C_6H_5CH_2 + H_2O$$

(Table IV summarizes rate expressions of the different reactions discussed in this work.)

Sensitivity analyses performed for toluene, under the same conditions (Fig. 16), show that among reactions influencing toluene oxidation there are ones resulting from its submechanism, and others from 1-hexene submechanism, competing for small reactive radicals. The more favoring reaction for toluene consumption is the decomposition of 1,3-C_6H_{11} (R1022). While the more inhibiting for toluene oxidation is the formation of the same radical (1,3-C_6H_{11}) through R1000. In fact, this radical can reform toluene as mentioned earlier, through reactions R1031 and R1032.

$$\text{R1022}: 1,3\text{-}C_6H_{11} = 1,3\text{-}C_4H_6 + C_2H_5$$

Finally, the added interaction reactions (R1031 and R1032) are among the reactions inhibiting the oxidation of the fuel components. Actually, these reactions reform toluene and transform hexenyl radicals into the less reactive hexadienes.

Ignition delay times of 1-hexene/toluene (30/70) mixture at 0.2 and 1 MPa were computed using the SENKIN code [50]. As can be seen from Fig. 17, the proposed kinetic mechanism overpredicts slightly the ignition delay times measured in a shock tube at both investigated pressure regimes. A better knowledge of the kinetic and thermodynamic parameters of hydrocarbons initiation reactions, and especially for toluene, would be very helpful for improving the modeling under these conditions, since the 1-hexene submechanism used here reproduces very well ignition delay times of pure 1-hexene at both 0.2 and 1 MPa [49]. Unlike for the modeling of the JSR experiments, the added cross-reactions do not affect the ignition delay time calculations, since the initiation steps are the most sensitive reactions. Sensitivity analyses for ignition delay times with respect of OH radical were performed at 1540 K under stoichiometric conditions and for the two pressures studied. Figure 18 presents the sensitivity analysis obtained for the binary mixture 1-hexene/toluene (30/70) at 0.2 MPa; note that the same reactions are present at high pressure 1 MPa. These analyses show that computed ignition delay times are accelerated by the branching reaction: Q3

$$\text{R6}: H + O_2 = OH + O$$

The second reaction favoring the mixture ignition is the decomposition of the benzyl radical formed by toluene:

$$\text{R770}: C_6H_5CH_2 = C_5H_5 + C_2H_2$$

Among the reactions that inhibit the mixture ignition, one can find reactions forming benzyl radical by H

Author Proof

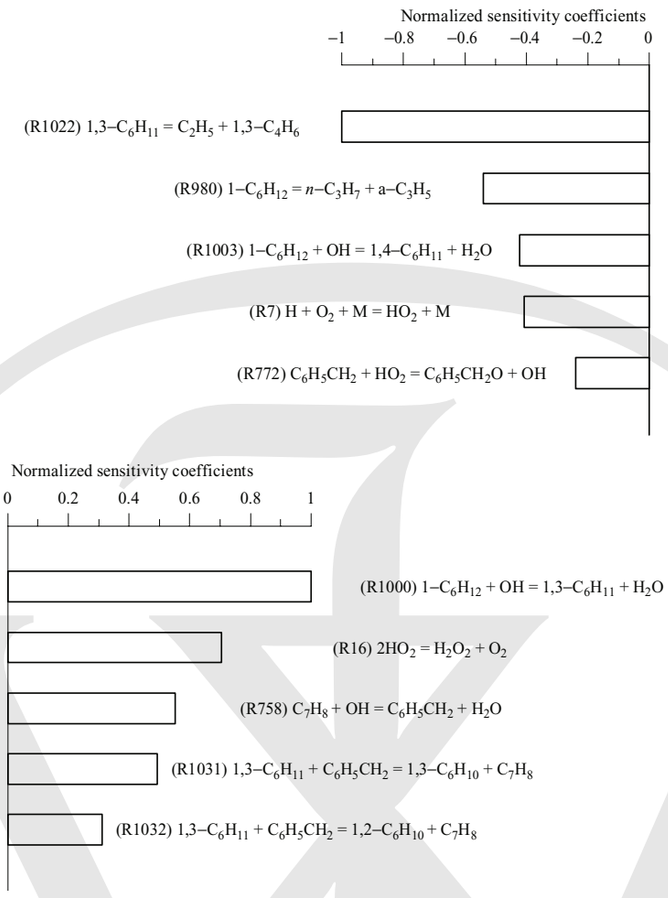

Figure 16 Sensitivity analysis of toluene consumption in the mixture 1-hexene/toluene (30/70) in a JSR, 0.1% fuel/0.9% O_2/99% N_2; $\tau = 0.5$ s; $\phi = 1$; $P = 1$ MPa; $T = 900$ K.

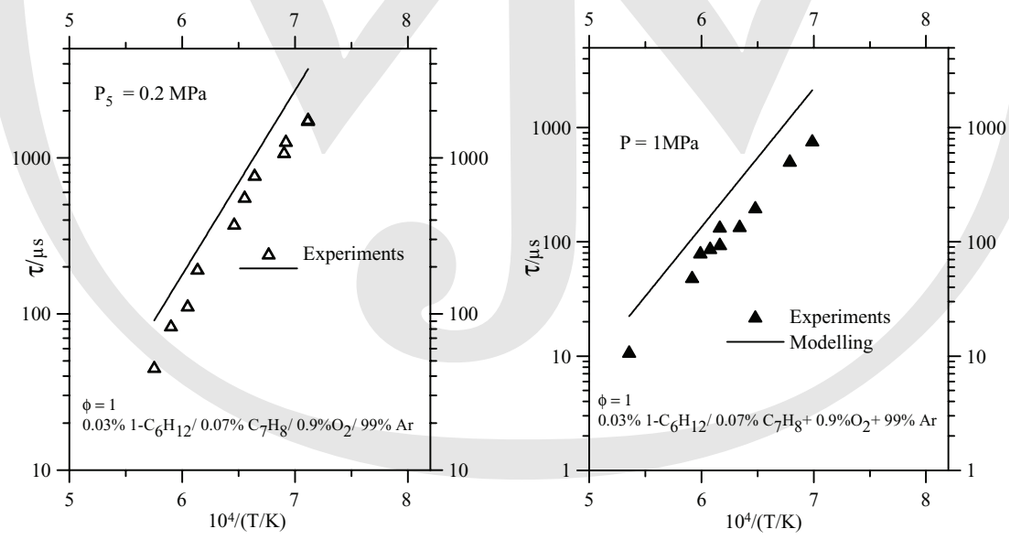

Figure 17 Comparison between experimental (symbols) and computed (curves) ignition delay times of a stoichiometric mixture 1-hexene/toluene (30/70) at 0.2 and 1 MPa. 0.1% fuel/0.9% O_2/99% Ar.

Author Proof

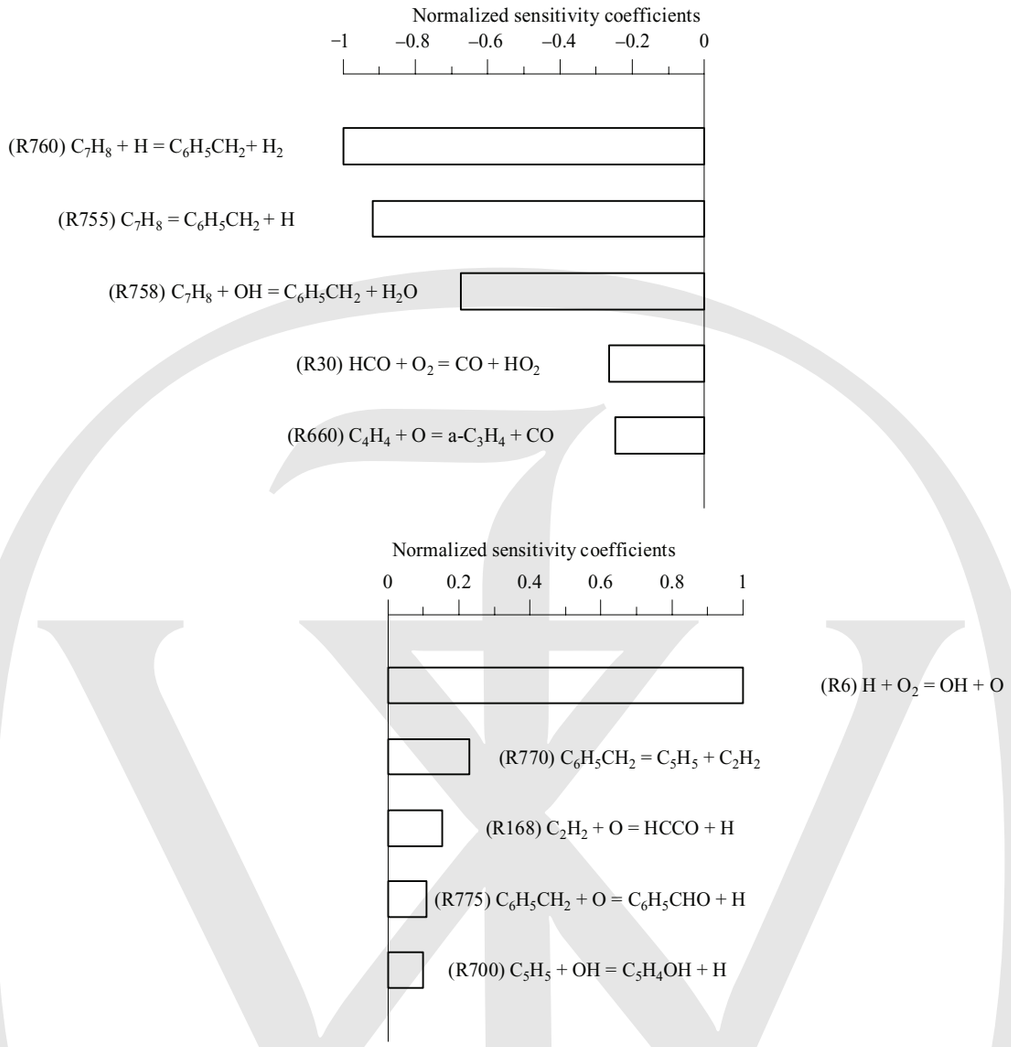

Figure 18 Sensitivity analysis for computed ignition delay times for the mixture 1-hexene/toluene (30/70) with respect of OH radical in a shock tube, 0.1% fuel/0.9% O_2/99% Ar; $\phi = 1$; $P_5 = 0.2$ MPa; $T = 1540$ K.

atom abstraction from toluene:

$$\mathrm{R760}: C_7H_8 + H = C_6H_5CH_2 + H_2$$

$$\mathrm{R755}: C_7H_8 = C_6H_5CH_2 + H$$

$$\mathrm{R758}: C_7H_8 + OH = C_6H_5CH_2 + H_2O$$

Binary mixture ignition delay times become long with increasing benzyl radical concentration in the mixture, so by increasing toluene mole fraction in the mixture composition, which agrees with our experiments (Fig. 2). We can also observe that no reaction from 1-hexene submechanism is present among the more sensitive reactions for the binary mixture ignition.

CONCLUSIONS

In the present work, the oxidation of several binary mixtures 1-hexene/toluene has been investigated, between 750 and 1860 K, under two pressures 0.2 and 1 MPa, and for three equivalence ratios 0.5, 1, and 1.5. The first part of experiments was carried out in a shock tube, and a new autoignition delay times database was obtained. Experiments in a shock tube demonstrated that binary mixture ignition delay times become long by increasing toluene mole fraction. The second part of this work was performed in a jet-stirred reactor, to measure species mole fractions of the binary mixtures at fixed residence time and variable temperature.

Author Proof

We showed that toluene reacts with common radicals at rates comparable to or greater than 1-hexene. 1-Hexene becomes less reactive when toluene is present, especially at temperature below 950 K, demonstrated by calculating its consumption rate. 1-Hexene consumption becomes partially unaffected by the presence of toluene at high temperature (>950 K), because 1-hexene is mainly consumed by thermal decomposition at this temperature range, so partially independent of small reactive radicals. Modeling results showed that the combination of the two hydrocarbons submechanisms is not sufficient to simulate experiments; cross-reactions between hydrocarbons are not limited to small common radicals, so other interaction reactions in which large radicals intervene are important.

Experiments performed using both a shock tube and a jet-stirred reactor were modeled using a detailed kinetic mechanism containing 159 species and 1242 reversible reactions. For JSR experiments, the computations when cross-reactions are taken into account in the model agree better with experiments at stoichiometric and rich equivalence ratio (except for acetylene), but this is not the case, for fuel-lean conditions for some species including CO, CO_2, CH_4, and C_2H_4. For shock tube experiments, no effect of cross-reactions was found and the model overpredicts slightly the measured ignition delay times of the investigated binary mixtures. Sensitivity analysis for both toluene and 1-hexene oxidation in a jet-stirred reactor showed that there are reactions from each hydrocarbon submechanisms as well as added crossreactions. Sensitivity analysis in a shock tube demonstrated that mixture ignition is inhibited by benzyl radical formed from toluene oxidation.

Flow diagrams of hydrocarbons showed that at low temperature (<900 K) 1-hexene as well as toluene are consumed by small reactive radicals, especially OH radical, to form 1,3-C_6H_{11} for 1-hexene and benzyl radical ($C_6H_5CH_2$) for toluene. For higher temperature (1100 K), 1-hexene is mainly consumed through its thermal decomposition to form n-C_3H_7 and a-C_3H_5, while toluene is consumed by OH, O, and H to form benzyl radical and also by displacement of a methyl group to form benzene.

BIBLIOGRAPHY

1. Dagaut, P. Phys Chem Chem Phys 2002, 4, 2079–2094.
2. Guibet, J. C. In Fuels & Engines, Vols. 1 and 2; Publications de l'Institut Français du Pétrole, Editions Technip, 1999.
3. Baker, J. A.; Skinner, G. B. Combust Flame 1972, 19, 347–350.
4. Dagaut, P.; Cathonnet, M.; Boettner, J.-C.; Gaillard, F. Combust Flame 1988, 71, 295–312.
5. Heyberger, B.; Belmekki, N.; Conraud, V.; Glaude, P. A.; Fournet, R.; Battin-Leclerc, F. Int J Chem Kinet 2002, 34, 666–677.
6. Dagaut, P.; Cathonnet, M.; Boettner, J.-C. J Phys Chem 1988, 92, 661–671.
7. Dagaut, P.; Cathonnet, M. Combust Sci Technol 1998, 137, 237–275.
8. Minetti, R.; Roubaud, A.; Therssen, E.; Ribaucour, M.; Sochet, L. R. Combust Flame 1999, 118, 213–220.
9. Ray, D. J. M.; Waddington, D. J. Combust Flame 1973, 21, 327–334.
10. Battin-Leclerc, F. Phys Chem Chem Phys 2002, 4, 2072–2078.
11. Bawn, C. E. H.; Skirrow, G. I. Proc Combust Inst 1955, 5, 77–84.
12. Tsang, W. Int J Chem Kinet 1978, 10, 1119.
13. King, K. D. Int J Chem Kinet 1979, 11, 1071.
14. Leppard, W. R. In International Fuels and Lubricants Meeting Exposition, Boston, Maryland, Sept. 25–28, 1989; SAE Technical Papers 892081.
15. Vanhove, G.; Ribaucour, M.; Minetti, R. Proc Combust Inst 2005, 30, 1065–1072.
16. Yahyaoui, M.; Djebaïli-Chaumeix, N.; Paillard, C.-E.; Touchard, S.; Fournet, R.; Glaude, P.-A.; Battin-Leclerc, F. Proc Combust Inst 2005, 30, 1137–1145.
17. McEnally, C. S.; Pfefferle, L. D. Combust Flame 2005, 143, 246–263.
18. Burcat, A.; Farmer, R. C.; Espinoza, R. L.; Matuala, R. A. Combust Flame 1979, 36, 313–316.
19. Burcat, A.; Snyder, C.; Brabbs, T. NASA Technical Memorandum 87312, 1986.
20. Pengloan, G. Ph. D. thesis, Université d'Orléans, 2001.
21. Eng, A.; Fittschen, C.; Gebert, A.; Hibmovschi, P.; Hippler, H.; Unterreiner, A. N. I. Proc Combust Inst 1998, 27, 211–218.
22. Venkat, C.; Brezinsky, K.; Glassman, I. Proc Combust Inst 1982, 19, 143–152.
23. Brezinsky, K.; Litzinger, T. A.; Glassman, I. Int J Chem Kinet 1984, 16, 1053–1074.
24. Brezinsky, K. Prog Energy Combust Sci 1986, 12, 1–24.
25. Emdee, J. L.; Brezinsky, K.; Glassman, I. J Phys Chem 1992, 96, 2151–2161.
26. Ristori, A.; Dagaut, P.; Pengloan, G.; El Bakali, A.; Cathonnet, M. Combustion 2001, 1, 265–294.
27. Davis, S. G.; Law, C. K. Combust Sci Technol 1998, 140, 427–449.
28. Johnston, R. J.; Farrell, J. T. Proc Combust Inst 2005, 30, 217–224.
29. Sivaramakrishnan, R.; Tranter, R. S.; Brezinsky, K. Proc Combust Inst 2005, 30, 1165–1173.
30. Astholz, D. C.; Durant, J.; Troe, J. Proc Combust Inst 1981, 18, 885–892.
31. Hippler, H.; Reihs, C.; Troe, J. Z Phys Chem Neue Folge 1990, 167, 1–16.
32. Colket, M. B.; Seery, D. J. Proc Combust Inst 1994, 25, 883–891.

Q4

Author Proof

33. Braun-Unkhoff, M.; Frank, P. Just, Th. Proc Combust Inst 1988, 22, 1053–1061.
34. Wilk, R. D.; Koert, D. N.; Cernansky, N. P. Energy Fuels 1998, 3, 292–298.
35. Filipe, D. J.; Li, H. L.; Miller, D. L.; Cernansky, N. P. SAE 920807, 1992.
36. Leppard, W. R. SAE 922325, 1992.
37. Dagaut, P.; Reuillon, M.; Cathonnet, M. Combust Sci Technol 1994, 103, 315–336.
38. Klotz, S. D.; Brezinsky, K.; Glassman, I. Proc Combust Inst 1998, 27, 337–344.
39. Andrae, J.; Johansson, D.; Björnbom, P.; Risberg, P.; Kalghatgi, G. Combust Flame 2005, 140, 267–286.
40. Vanhove, G.; Petit, G.; Minetti, R. Combust Flame 2006, 145, 521–532.
41. Curran, H. J.; Pitz, W. J.; Westbrook, C. K.; Callahan, C. V.; Dryer, F. L. Proc Combust Inst 1998, 27, 379–387.
42. Glaude, P-A.; Conraud, V.; Fournet, R.; Battin-Leclerc, F.; Côme, G.; Scacchi, G.; Dagaut, P.; Cathonnet, M. Energy Fuels 2002, 16, 1186–1195.
43. Tanaka, S.; Ayala, F.; Keck, J. C. Combust Flame 2003, 133, 467–481.
44. Naik, C. V.; Pitz, W. J.; Sjöberg, M.; Dec, J. E.; Orme, J.; Curran, J. M.; Simmie, J. M.; Westbrook, C. K. In Joint Meeting of the US Section of The Combustion Institute, Philadelphia, PA, Mar., 20–23, 2005.
45. Paillard, C.-E.; Youssefi, S.; Dupré, G. Prog Astronaut Aeronaut 1986, 105, 394–406.
46. Dagaut, P.; Cathonnet, M.; Rounan, J. P.; Foulatier, R.; Quilgars, A.; Boettner, J. C.; Gailard, F.; James, H. J. Phys E: Sci Instrum 1986, 19, 207–209.
47. Simmie, J. M.; Rolland, S.; Ryder, E. Int J Chem Kinet 2005, 37, 341–345.
48. Bittker, D. A. NASA Technical Memorandum 102443, 1990.
49. Yahyaoui, M.; Djebaïli-Chaumeix, N.; Dagaut, P.; Paillard, C.-E.; Gail, S. Combust Flame 2006, 147, 67–78.
50. Lutz, A. E.; Kee, R. J.; Miller, J. A. Sandia Report SAND87-8248UC-401, 1992.
51. Glarborg, P.; Kee, R. J.; Grcar, J. F.; Miller, J. A. Sandia National Laboratories Report, SAND86-8209, Livermore, CA, 1986.
52. Kee, R. J.; Rupley, F. M.; Miller, J. A. Report no. SAND87-8215, Sandia National Laboratories, 1991. Q5

Author Proof

Queries

Q1: This is the usual format to acknowledge direct financial support. Spell out acronyms and confirm that these are separate grant sponsors and that the wording of each is correct.
Q2: Provide the symbols of the units used in the footnote of Table IV.
Q3: Confirm whether citation of Fig. 18 is OK here.
Q4: Provide the location of the publisher.
Q5: Confirm whether initials of the third author are OK as set.

WILEY InterScience® DISCOVER SOMETHING GREAT